Whole Body and Local SAR in Anatomical Phantoms Exposed to RF Fields from Birdcage Coils

Eugenia Cabot[1], Andreas Christ[1], Niels Kuster[1,2]

[1]Foundation for Research on Information Technologies in Society, Zeughausstr. 43, 8004 Zurich, Switzerland
e-mail:cabot@itis.ethz.ch
[2]Swiss Federal Institute of Technology (ETH), 8092 Zurich, Switzerland

Abstract

A numerical study of the induced fields and specific absorption rate (SAR) in anatomical phantoms exposed to the radiofrequency (RF) fields of magnetic resonance (MR) scanners was conducted using the finite difference time domain (FDTD) method at 64MHz and 128MHz. Three phantoms including two adults and one child were used. The study revealed inconsistencies between the MRI safety standards and current scanning practices. Furthermore, the results indicate that established guidelines for demonstrating MRI safety of implants are insufficient.

1. Introduction

The current designs of Magnetic Resonance (MR) scanners use steadily increasing magnetic field strengths which correspond to the rise of the Larmour frequency of RF fields. Scanners which operate at 1.5T or 3T use frequencies of 64MHz or 128MHz. At these frequencies, the field distribution in the body of the patient is highly inhomogeneous. In order to protect the patient from excessive tissue heating, MR safety standards, such as [1], [2] and [3] define limits for the whole body SAR and for the peak spatial average SAR (hot spots) for various operational modes of the MR scanner. During examinations, only the whole body SAR of the patient is controlled by the MR scanner or clinical personnel. The assessment of local hot spots during clinical routine procedures is not feasible. The reliable assessment of the local SAR, which can contribute to tissue heating, is a prerequisite for patient safety. In particular for the evaluation of safety of metallic medical implants the incident field conditions need to be known. Current testing safety standards, such as [4]. do not consider the high inhomogeneities of the incident fields which become increasingly complex at higher frequencies, because the wavelengths in the tissues reach the order of magnitude of the dimensions of the anatomical features of the body.

2. Objectives

The main objective of this study is to characterize numerically the local and the whole body absorption in patients undergoing MR examinations as a function of RF frequency, patient size, weight, tissue distribution and position in the birdcage coil and to assess whether it is possible to correlate the whole body absorption in the patient with local exposure. This includes:

- the assessment of local and whole body SAR in the human body when exposed to the RF-fields of a birdcage coil for various configurations,
- the characterization of tissue distributions and incident fields which lead to local hot spots and possible tissue heating,
- the identification of the local SAR or the whole body SAR as a limiting factor of the exposure
- the discussion of the observed effects on possible consequences on implant heating and on implant safety testing

3. Methods

The SAR distributions in various human body models of adults [5], [6] and a child [7] were simulated in generic birdcage coils at frequencies of 64MHz and 128MHz using the FDTD method and the simulation platform SEMCAD X. In addition the whole body SAR (SARwb) and the 10g and 1g peak spatial average SAR (SAR10g and SAR1g) were calculated. The required grid resolution for the anatomical models was assessed using a series of continuously refined simulations. A resolution of $2x2x2mm^3$ inside the anatomical models yields consistent results.

3.1 Numerical Model of the Birdcage

The birdcage was modeled as a 16-rung with a diameter of 620mm and a length of 650mm. It was tuned to resonance frequencies of 64MHz and 128MHz by adjusting the capacitors in its end rings to 63.5pF and 12pF, respectively. In order to reduce the simulation time required for steady state at the operating frequencies, an alternative

feeding was used: current sources were placed directly into the center of the rungs, enforcing the current distribution in the cage to achieve the necessary highly homogeneous B_1-field.

3.2 Anatomical Models

The adult male model is based on cryosection images provided from the 'Visible Human' project [6] of an individual being 1.80m and 98kg. The resolution along the body axis is 2mm (1mm in the head). The Visible Human is composed by more that 100 tissue regions and organs. The adult female model [5] is based on MRI scans of a 22 year old female of 1.60m and 53kg. The model voxel size is $2x2x2mm^3$ and consists of more than 50 tissue regions and organs. The 6-year-old child is one of the models developed in the Virtual Family project [7]. The model is based on high resolution MR-images.

4. Results

This section is organized as follows: first results for 1.5T coil are shown, for 3 different anatomical phantoms in a single position and then for the female phantom in different landmarks. Then, results for 3 the different anatomical phantoms at 3T. All the results obtained from the simulations are normalized to the B_1 at the center of the birdcage coil. In addition results are also interpreted in terms of safety guidelines [2].

4.1. SAR in the Different Anatomical Models at 1.5T

The SARwb, as well as the SAR1g and SAR10g were first computed for three different phantoms (adult male, adult female and child) centered inside the birdcage coil, with their shoulders at the level of the upper ring, see Fig 1. This position is the one allowing the maximum volume exposure to the coil fields. Results are summarized in Table 1.

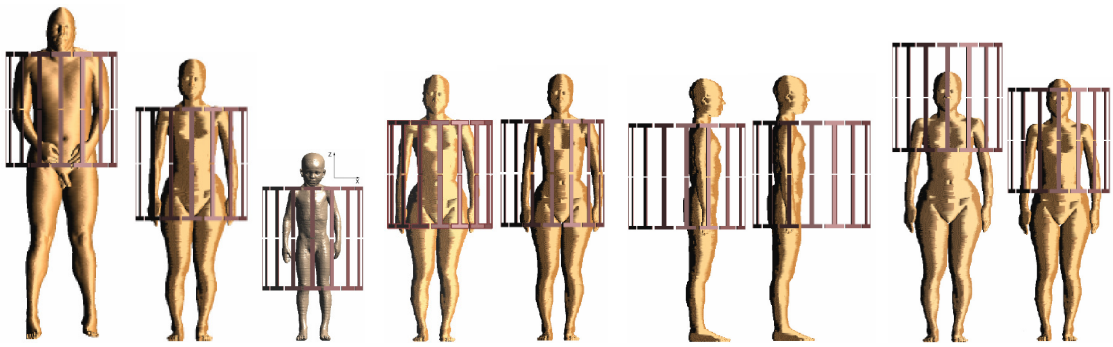

(a) Section 4.1 and 4.3. **(b) Section 4.2.1.** **(c) Section 4.2.2.** **(d) Section 4.2.3.**

Fig 1. Landmarks of the anatomical phantoms inside the birdcage. The 3 positions on the left are used in section 4.1 and section 4.3, the next 2 positions are used in section 4.2.1, the following 2 positions correspond to section 4.2.2 and the 2 last positions are commented in section 4.2.3.

Table 1. Whole body SAR, 1g and 10g averaged Peak Spatial SAR for the adult male, the adult female and the child phantoms in the centered position. The values are scaled to 1μT in the isocenter of the coil.

	Adult Male	Adult Female	Child
SARwb [W/kg/μT^2]	0.18	0.13	0.077
SAR1g [W/kg/μT^2]	3.6	3.2	0.89
SAR10g [W/kg/μT^2]	2.4	2.1	0.69

All values are normalized to a B_1 field of 1μT. The whole body SAR values in this position range from 0.077W/kg in the child to 0.18W/kg in the adult male. The maximum SAR1g ranges from 0.89 to 3.6W/kg. Scaling the SAR1g value to the SARwb limit of 4W/kg (first level controlled mode) [2] translates into a maximum SAR1g of 80W/kg, 98W/kg, and 46W/kg for the adult male, adult female and child, respectively, which significantly exceeds the exposure limit of 8W/kg for the SAR1g (first level controlled mode).

Hot spots can be seen in the limbs, especially where the arms are close to the body, and at the groin. Generally, hot spots are likely to occur at tissue interfaces with high dielectric contrast (e.g., fat and muscle tissue). Similar

patterns have been observed in all 3 phantoms. For instance, hot spots are formed in muscle tissue located between the rib bones in all 3 cases. Examination of the SAR throughout the adult female model showed that hot spots exist in highly conductive tissue, like muscle, but also in tissue interfaces such as fat-muscle, kidney-liver and fat-uterus. Fig 2 shows the SAR1g distribution in two coronal slices of the adult female and the adult male. Hot spots can be seen in the limbs, in muscle tissue and in tissue interfaces like muscle and fat.

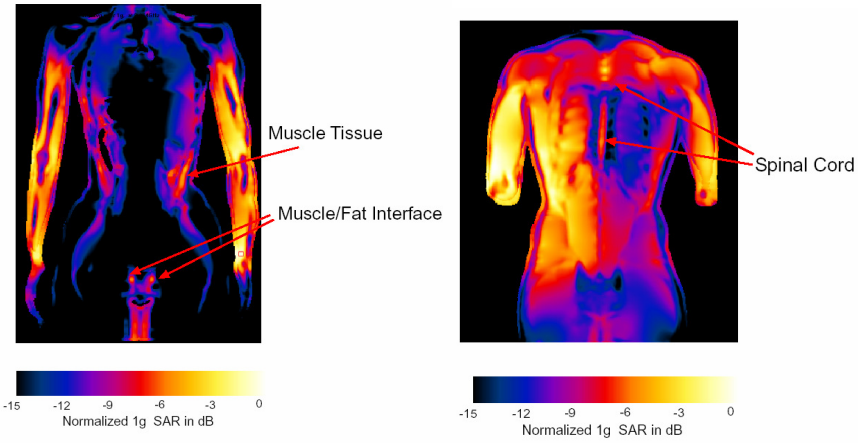

Fig 2. SAR1g extracted in two coronal slices. Hot spots are observed in high conductive tissues, like muscle and the spinal cord, and also in tissue interfaces.

4.2. SAR in Different Positions of the Female at 1.5T

In order to evaluate the influence on the power absorption of the body location inside the coil, several simulations were performed for a given phantom (adult female) in various positions. The phantom was shifted in three directions, left/right (x-direction), up/down (y-direction) and along the coil axis (z-direction).

4.2.1. SAR in Female: x-Translation

First, the phantom was moved in the x-direction, i.e., to the left and to the right of the original position see (Fig 1 (b)), with no variation in the other directions. Through this movement the phantom approaches the rungs of the coil. Because of the radial increase of the E-fields in the cage the SARwb increases by 15% in comparison to the centered position. This is the case for the two x-translations, x1 and x2 (Fig 1 (b)). The SARwb remains the same for the two off-centered positions, but there are differences in the local SAR. In both cases the maximum SAR1g is produced in the one arm that is closer to the legs. In one position the SAR1g is 3.9W/kg, and in the other it reaches 4.9W/kg. Scaling this value to the exposure limit of SARwb=4W/kg [2], the SAR1g can exceed 130W/kg. The SAR values are summarized in Table 2.

4.2.2. SAR in Female: y-Translation

The phantom was then moved in the y-direction (up and down, see Fig 1 (b)). The translations bring the body closer to the rungs of the coil. The SAR levels are expected to rise, assuming a linear and radially growing E-field. The SARwb reached 0.22 W/kg. The maximum SAR1g was produced in both positions in the right arm, in the muscles or muscle-to-fat interface at the level of the wrist in the first position and the level of the elbow in the second one. The SAR1g can reach 7.4W/kg. Scaled to the 4W/kg [2] limit this would result in a SAR1g beyond 130W/kg, approximately the same value obtained with the x-translation. A summary of these values can be found in Table 2.

4.2.3. SAR in Female: z-Translation

The phantom was also moved along the axis of the birdcage coil, see Fig 1(d). The SARwb decreases, especially when the head is centered in the coil, to 0.01W/kg, since only a small proportion of the body is exposed. It is worth mentioning that in the two first translations, the shoulders and the neck are exposed to the birdcage coil fields, and the maximum local SAR is produced in both cases at the shoulder-neck arc. These values are collected in Table 2.

Table 2.Whole body SAR, 1g and 10g averaged Peak Spatial SAR for the adult female in four off-centered positions: y direction and z direction. The values are scaled to 1μT in the isocenter of the coil.

	x1	x2	y1	y2	z1	z2
SARwb [W/kg/μT^2]	0.15	0.15	0.16	0.22	0.01	0.06
SAR1g [W/kg/μT^2]	3.9	4.9	3.7	7.4	0.57	1.1
SAR10g [W/kg/μT^2]	2.6	3.5	2.5	5.2	0.41	0.88

4.3. SAR in the Different Anatomical Models at 3T

The SARwb, as well as the SAR1g and SAR10g were first computed for three different phantoms (adult male, adult female and child) centered inside the birdcage coil, with their shoulders at the level of the upper ring, see Fig 1. Results are summarized in Table 3.

The SARwb values in this position range from 0.31W/kg in the adult male to 0.41W/kg in the child. The maximum SAR1g ranges from 4.8 to 5.3 W/kg.

Table 3. Whole body SAR, 1g and 10g averaged Peak Spatial SAR for the adult male, the adult female and the child phantoms in the centered position inside the 3T birdcage coil. The values are scaled to 1μT in the isocenter.

	Adult Male	**Adult Female**	**Child**
SARwb [W/kg/μT^2]	0.31	0.24	0.41
SAR1g [W/kg/μT^2]	5.2	5.3	4.8
SAR10g [W/kg/μT^2]	3.9	3.9	3.7

5. Discussion and Conclusions

The simulations have shown that the local SAR limits be significantly exceeded when the patient is scanned at the whole or partial body exposure limits. The maximum SAR1g and SAR10g are likely to occur in the limbs, because of the increase of the E-field in radial direction of the bore axis.The maximum values in the trunk appear in a highly conductive tissue as muscle and also in fat-muscle interface Approaching the body to the coil rungs could increase the SAR1g up to a 50%, whereas translation of the body in the z direction does not necessarily change the position of the maximum: if the neck-shoulder arc is not outside the coil, the maximum value will appear there, suggesting that the shape and dielectric distribution of the model has a big impact on the SAR distribution.

The local enhancements of the incident electrical field which are due to the inhomogeneities of the dielectric properties of the body tissues will directly affect the currents induced on metallic implants. Present standards for the MR safety testing of such implants use homogeneous body phantoms which do not reproduce these effects and can therefore strongly underestimate the heating caused by the induced currents.

6. References

1. U.S. Food and Drug Administration (FDA). *Criteria for significant risk investigations of magnetic resonance diagnostic devices. 2003.*
2. International Electrotechnical Commision (IEC). *IEC 60601-2-33 Medical electrical equipment –Part 2-33: Particular requirements for the safety of magnetic resonance equipment for medical diagnosis.* International Electrotechnical Commission, 3, rue de Varemb, PO Box 131, CH-1211 Geneva 20, Switzerland, 1999.
3. ICNIRP. International Commission on Non-Ionizing Radiation Protection, medical magnetic resonance (MR) procedures: Protection for patients. *Health Physics,* 87(2):197-216, 2004.
4. ASTM International, Standard F218202a, Standard Test Method for Measurement of Radio Frequenczy Induced Heating Near Passive Implants During Magnetic Resonance Imaging, www.astm.org.
5. Tomoaki Nagaoka et al. Development of realistic high-resolution whole-body voxel models of Japanese adult males and females of average height and weight, and application of models to radio-frequency electromagnetic-field dosimetry. *Physics in Medicine and Biology,* 49 (1):1-15, January 2004.
6. Michael J. Ackerman. The Visible Human Project. *Proceedings of the IEEE*, 86 (3): 504-511, March 1998.
7. A. Christ et al., The Virtual Family – Development of anatomical CAD models of two adults and two children for dosimetric simulations, in preparation.